

Profitability optimization of a wind power plant performed through parabolic RANS simulations and an economic model

V. Santhanagopalan, L.Y. Al-Hamidi, S. Letizia, L. Zhan and G. V. Iungo The University of Texas at Dallas, Mechanical Engineering Department, 75080 Richardson, TX

This work focuses on the optimization of performance and profitability of a wind farm carried out by means of an economic model and Reynolds-Averaged Navier-Stokes (RANS) simulations of wind turbine wakes. Axisymmetric RANS simulations of isolated wind turbine wakes are leveraged with a quadratic super-positioning model to estimate wake interactions within wind farms. The resulting velocity field is used with an actuator disk model to predict power production from each turbine in the wind farm. Design optimization is performed by considering a site in North Texas, whose wind resource statistics are obtained from a meteorological tower. The RANS solver provides capabilities to simulate different incoming wind turbulence intensities and, hence, the wind farm optimization is performed by taking the daily cycle of the atmospheric stability into account. The objective functional of the optimization problem is the levelized cost of energy (LCoE) encompassing capital cost, operation and maintenance costs, land cost and annual power production. At the first level of the optimization problem, the wind farm gross capacity is determined by considering three potential turbine types with different rated power. Subsequently, the optimal wind farm layout is estimated by varying the uniform spacing between consecutive turbine rows. It is found that increasing turbine rated power, the wind farm profitability is enhanced. Substituting a wind farm of 24 turbines of 2.3-MW rated power with 18, 3-MW turbines could reduce the LCoE of about 1.56 \$/MWh, while maintaining a similar gross capacity factor. The optimization of the spacing between turbine rows was found to be sensitive to the land cost. For a land cost of 0.05 \$/m², the layout could be designed with a spacing between 6 to 15 rotor diameters without any significant effect on the LCoE, while an increased land cost of 0.1 \$\frac{1}{m^2}\$ leads to an optimal spacing of about 6 rotor diameters.

I. Introduction

Wind farm design and optimization (WFDO) is a complex, non-linear interdisciplinary problem.¹ The WFDO framework encompasses a detailed description and evaluation of the wind farm profit, which has to be maximized through different optimization variables and algorithms.² The performance of a wind farm can be quantified through power capture of the wind turbines, without disregarding the curtailed durability of the wind turbines and additional costs associated to sub-optimal operational conditions. The performance can be factored with different costs encountered during the life cycle of the wind farm in order to estimate the actual profit. A common detrimental factor of wind farm performance is connected with wake interactions between the turbines, which result in curtailed power production and added fatigue loads due to the wake-generated turbulence.³

Profitability of a wind power plant is typically quantified through a multi-objective functional, which encompasses power production of the wind turbines accounting for wake interactions, capital costs associated with the type and number of turbines, land cost varying for different locations and farm size, regular operation and maintenance costs, and the effects of fatigue loads on increased maintenance costs. The metrics most widely used to quantify wind farm performance and profit are the Annual Energy Production (AEP) and the Levelized Cost of Energy (LCoE).¹

Once a suitable objective functional is formulated, its optimization is a non-trivial task due to its non-convex nature for variations of the different design and control parameters, such as number of wind turbines in the array, land area, site complexity, wind resource statistics, wind turbine positions, rotor diameter, d,

tip speed ratio $(TSR = \omega_{rot}d/(2 U_{\infty}))$, where ω_{rot} is the rotor angular velocity and U_{∞} is the incoming hub-height wind velocity).

For WFDO problems, the wake flow within the wind farm, turbine power capture and fatigue loads are typically estimated for a large number of farm configurations, wind speed and direction. Subsequently, fast computation is the highest priority in the various characteristics of the solver used for wind farm simulations. This justifies the frequent use of engineering and analytical wake models for WFDO problems. A numerical tool featuring capability of simulating different conditions of the incoming wind turbulence and turbine operative conditions without adversely increasing the computational cost, would improve the reliability of the optimization solver. To this aim, a RANS-based solver simulating wind farm flow field for different incoming wind turbulence has been recently proposed.^{7,8} The computational costs of this solver are comparable to those of engineering wake models, due to the boundary layer and axisymmetry assumptions for the wake flow, and a parabolic approximation for the solution of the RANS equations (P-RANS solver).^{8–10}

Ref.⁸ showed applications of P-RANS in performance optimization of a wind turbine column, where power capture and fatigue loads were included in the objective functional of the optimization problem. It was shown how important incoming turbulence intensity is for the wind farm optimization problem. In this paper, we propose to expand this application to a more robust economic model, which considers typical costs associated with the wind energy industry. Specifically, LCoE is used as the objective functional, and the optimization is performed to determine multiple variables in design and operation of a relatively small wind farm. While the P-RANS has significantly small computational cost, it uses the axisymmetric approximation for the wake flows. In order to estimate the wind farm performance for multiple wind directions, a wake superposition method is then applied.^{11,12}

The remainder of this paper is structured as follows: in the next section, the P-RANS solver is summarized, while in Sect. III the objective functional, strategy and framework of the optimization problem are presented. Subsequently, the results obtained from this WFDO problem are discussed in Sect. IV. Finally, concluding remarks are reported in Sect. V.

II. Parabolic RANS solver and wind farm wake model

For this study, a parabolic RANS solver is used for simulations of wakes produced by wind turbines.^{7,8} The RANS equations for incompressible and axisymmetric flows are solved with a parabolic approximation, i.e., by advancing the flow solution in the downstream direction and neglecting the elliptic nature of subsonic flows. 13 This strategy enables accurate predictions of the flow past wind turbines with computational costs curtailed by about two orders of magnitude compared to global 3D RANS solvers.^{7,8} Reynolds stresses in the RANS equations are modeled using the Boussinesq hypothesis 14 and the turbulence closure is achieved through a one-equation model, where the parabolic-transport equation for turbulent kinetic energy is solved with a calibrated mixing length to estimate the turbulent eddy-viscosity. This strategy allows determining effects of incoming freestream turbulence on the wake velocity field. The eddy-viscosity in downstream induction zone of the first turbine is estimated as a constant, $\nu_{t,1} = c_{\mu}^{1/4} l^* \sqrt{3/2} (T I_{inc} U_{\infty})$, where c_{μ} is model constant of value 0.09, $T I_{inc}$ is the incoming turbulence intensity and l^* is a length scale calibrated to be equal to 0.1. Everywhere else, the calibrated mixing length is used with the Prandtl-Komogorov expression to determine the eddy-viscosity as $\nu_{t,i} = c_{\mu}^{1/4} l_m(x) \sqrt{k(x,r)}$, where k is the turbulent kinetic energy. 14 This CFD tool is meant to be a valid alternative to engineering models for prediction of wind turbine wakes, such as the Jensen model⁴ or the more recent Gaussian model,⁵ while providing the capability of simulating effects of incoming turbulence and wake-generated turbulence on downstream evolution of wind turbine wakes and power production.

The reference wind turbine used in this work is the 5-MW NREL, which has a rotor diameter of 126 m and hub height of 90 m. Aerodynamic forcing exerted by the turbine blades on the incoming wind is reproduced by using the actuator disc model. Since the solver employs non-dimensional parameters, the turbine can be scaled for different rated powers. The local angle of attack of the turbine blades and velocity magnitude as a function of the radial position are estimated through an iterative procedure in the parabolic code. The local lift and drag coefficients are calculated at each iteration through look up tables. Aerodynamic loads at tip and root of the blades are corrected through a modified Prandtl correction factor to take effects of vortices into account. For a different turbine rating, the geometric and aerodynamic characteristics of this turbine are scaled by simply varying the rotor diameter.

At the inlet, the incoming velocity field is imposed as Dirichlet boundary condition, axisymmetry condi-

tions are imposed at the turbine axis for the three velocities in cylindrical coordinates and pressure, while at the lateral boundaries null Neumann conditions are imposed for velocities and pressure. The RANS equations are discretized in the radial direction by using a Chebyshev pseudospectral collocation method implemented in Matlab. The numerical grid is mapped typically with 21 points over the rotor radius, which was determined through a previous grid sensitivity study. The parabolic equations are marched in the streamwise direction by using an explicit Euler method, which is equivalent to a forward first-order finite-difference scheme. The P-RANS solver is publicly available on GitHub at https://github.com/UTD-WindFluX/P-RANS.

For determining the entire wind farm performance, the wake velocity field of an isolated turbine obtained through the RANS solver is coupled with a wake superposition method that accounts for partial and full wake interactions among different turbines in the wind farm. The velocity at any location of the wind farm, U_x^{eff} , is determined as:^{11,12}

$$\frac{U_x^{eff}}{U_\infty} = 1 - \sqrt{\sum_{m=1}^{N_{wt}} \left(1 - \frac{U_x^m}{U_\infty}\right)^2} \tag{1}$$

where N_{wt} is the total number of turbines and U_x^m is the streamwise velocity field obtained from the P-RANS simulation of the m^{th} isolated turbine. Using the effective wake field obtained through the superposition method, U_x^{eff} , the individual turbine performance is re-estimated by calculating the aerodynamic forces acting on the rotor through the actuator disc model with blade element momentum theory. Partial wake interactions are treated by using the azimuthal averaging of the velocity field at different radial positions. The power capture of the i-th turbine, P_i , is obtained from the aerodynamic tangential force per unit area, $F_{tang,i}$, as:

$$P_i = \int_0^R 2\pi B\omega r^2 F_{tang,i}(r)dr \tag{2}$$

where B is equal to 3 representing the number of blades of the turbine rotor.

III. Optimization framework and mixed-objective functional

In this work, the WFDO problem is split into two levels, which are solved consecutively. The variables considered at the first optimization level are the rated power and the total number of wind turbines, with the constraint of using the same turbine type throughout the entire wind farm. Two different values of the incoming turbulence intensity are considered to mimic different regimes of the atmospheric stability, namely 5% and 15% for stable and convective conditions, respectively.⁸

At the second level of the optimization problem, the uniform spacing between the turbine rows is optimized by minimizing LCoE. Wind sectors of the wind rose with 10° width are evaluated by averaging the power production with a 1° resolution within each wind sector. Subsequently, wind speed bins are evaluated, while region-3 operations of the turbines are simply treated by limiting the maximum power production from the turbines to the rated power. Calculations are performed separately for stable and convective regimes in order to determine the significance of the atmospheric stability on the overall wind farm performance.

In analogy to a wind farm in North Texas investigated in El-Asha *et al.* 2017,³ a turbine array of three rows is considered for this work, for a total of 24 turbines with a rated power of 2.3 MW, rotor diameter, *d*, of 108 m and hub height of 80 m. For this site, the wind resource is dominated by southerly wind directions (WD); indeed, about 40% of the available wind occurred for the wind sector between 150° and 210°, where WD=180° represents direction from south to north.

The wind data collected from the met-tower are clustered into two stability regimes, namely the convective and the stable regimes. This is done by using as threshold a shear exponent value of 0.15 to distinguish the two regimes.^{3,20} Figures 1a and b show the wind rose for stable and convective regimes, respectively. Wind conditions during the stable regime have higher probability of wind speeds greater than the turbine rated speed, while turbines would operate mainly in region 2 of the power curve during convective conditions.

The objective functional of the WFDO problem is LCoE, which has to be minimized in order to maximize the wind farm profitability. The LCoE is defined as:

$$LCoE = \frac{FCR \times \sum_{j=1}^{N_{wt}} (C_{wt,j} + C_{elec,j}) + N_{wt} \times (C_{land} + C_{oper} + C_{main})}{AEP}$$
(3)

where N_{wt} is the number of wind turbines in the array, $C_{wt,j}$ is the cost of the j-th wind turbine, which includes nacelle-rotor assembly and supporting structures. C_{land} is the annual leasing cost of land per

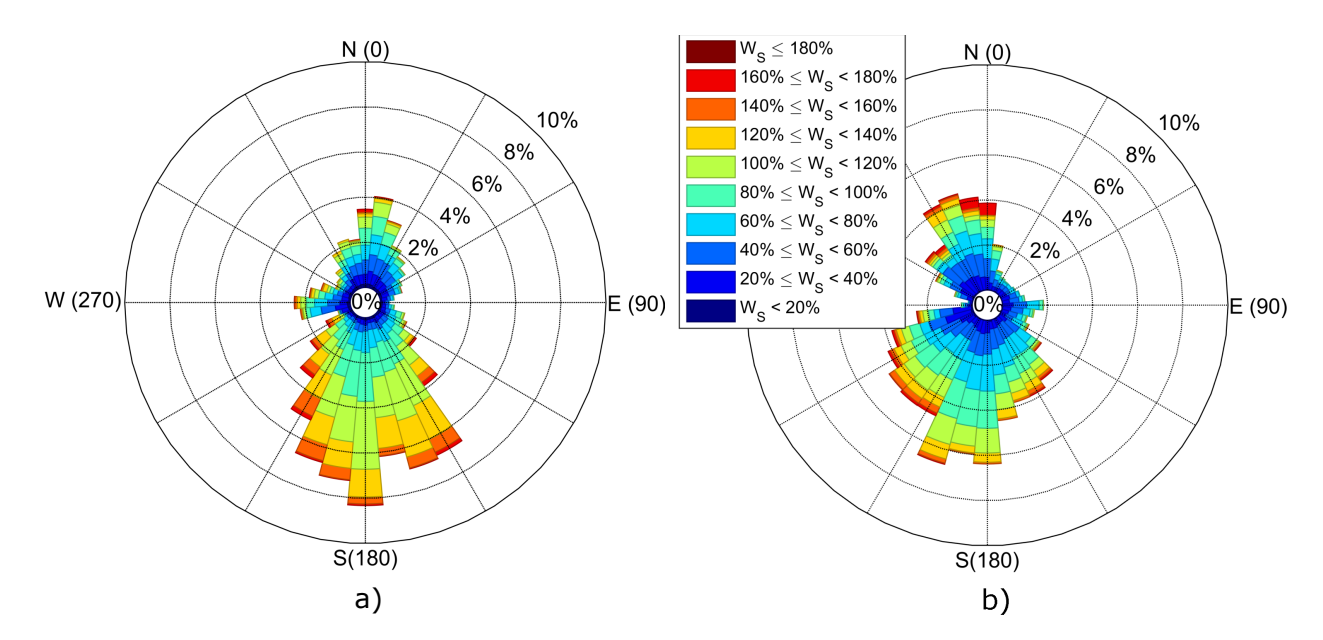


Figure 1. Wind rose of the hub-height velocity as percentage of the turbine rated speed: a) stable conditions; b) convective conditions.

turbine, $C_{elec,j}$ is the cost of electrical connections for power transmission associated to each turbine, C_{oper} is the annual operational cost and C_{main} is annual cost per turbine due to maintenance. FCR is fixed rate charge, which is an economic parameter representing the annual charges associated to the capital costs considering different financial aspects from the economic life of the wind farm.

The cost model for onshore wind farms installed in 2015 is used in this study.²¹ In level 1 of the optimization problem, the diameter of the turbine, d, affects various components of the capital costs $C_{wt,j}$, namely tower, foundation, assembly and installation costs. A scaling of the design costs is applied for the three different sizes of turbines, d_j .^{21,22} The total number of turbines, N_{wt} , affects all components of the total capital costs, while the spacing between turbines affects only C_{land} . However, all the variables in this optimization study affect the power production from the wind farm, AEP. The nacelle-rotor assembly, electrical costs, maintenance and operational costs are assumed to be dependent only on the rated power of the turbine. The cost components and the scaling model are explained in more detail in the Appendix.

As mentioned above, the WFDO problem is split in two levels. At the first level the number of turbines, N_{wt} , and the corresponding turbine rating, thus the turbine rotor diameter d, are optimized. Three turbine ratings are considered, namely 1.7 MW, 2.3 MW and 3 MW, which lead to rotor diameters, d, of 87.9 m, 97.2 m and 106.3 m, respectively. Hub height is fixed to 80 m.

To determine the wind farm rated power, P_{farm}^{rated} , a target is fixed in the range between 54 to 57 MW. As typical for wind farm problems, an aligned layout is adopted in this work. As baseline case, a layout with 3 rows with a streamwise spacing of 14.5 d and spanwise spacing of 3.3 d is considered. It results that the number of turbines required to match the wind farm rated power is equal to 33, 24 and 18 for turbine ratings of 1.7 MW, 2.3 MW and 3 MW, respectively.

At the second level of the optimization problem, the uniform streamwise spacing between consecutive rows, s, is optimized in order to obtain the optimal trade-off between AEP and land cost. A minimum streamwise spacing between two consecutive turbines of 4 d_j is constrained for the optimization problem. In level 2 of the optimization problem, the LCoE is minimized as function of the streamwise spacing, s, through a heuristic approach.

IV. Results

Table 1 shows the results from level 1 of the optimization problem for a land cost of 0.05 \$/m². Wake loss is defined as the power loss due to wake interactions as a ratio of total gross power available for the wind farm. The Case 1 consists of 24, 2.3-MW turbines deployed with an aligned configuration with streamwise

AEP (MWh/ Wake Loss Wake Loss Wake Loss AEP LCoE $P_{rated}^{farm}(\mathrm{MW})$ $P_{rated}^{turbine}(MW)$ Case N_{wt} Stable (%) Convective (%) Total (%) (GWh) MW/yr) (\$/MWh) 1 2.3 24 55.22.2%1.8% 4.0%278.30 5041.749.34 1.7 33 56.1 2.4%1.9% 4.3%282.19 5030.1 51.422 3 1.7 24 40.8 2.2%1.8% 4.0%205.70 5041.7 51.30 4 3.0 18 54.0 2.1%1.7%3.8%273.015055.747.78 5 3.0 24 72 2.2%1.8%4.0%363.00 5041.7 47.91

Table 1. Level 1 of the optimization problem for different turbine rated power and wind farm gross power.

spacing of 14.5 d and spanwise spacing of 3.3 d. For the Case 1, an overall wake loss of 4% is estimated.^{3,24} The wake loss associated with the stable regime is higher than for the convective regime, namely 2.2% and 1.8%, respectively. The overall probability of wind occurring in stable and convective regime are 49% and 51%, respectively. The windrose used in this work represents data measured for one year, in contrast with the dataset covering only three months used in El-Asha et al. 2017,³ where the effects of wake losses were estimated to be much larger under stable conditions (4%) than for convective conditions (2.4%). The results presented for this study are clearly justified by the windrose shown in Figure 1. Wind speeds higher than rated velocity occur typically under stable regimes. Therefore, even in presence of wake interactions, turbines will keep operating at the rated power. In contrast, for operations in region 2 of the power curve, wake interactions entail systematic under-performance of downstream wind turbines.

To explain more in detail the obtained results, the comparison of percentage power loss is reported in Figure 2 for different atmospheric stability regimes and wind sectors. The percentage power loss is defined as the power that would be lost due to wake interactions normalized by the available power.³ Figure 2a shows percentage power loss by considering the entire wind rose. The percentage power loss under stable regime, which is represented with dashed bars, is larger than during the convective regime confirming results from previous investigations.^{3,24} The turbines at the center of the wind farm experience higher percentage power loss due to wakes generated from the neighbor wind turbines for any the wind direction.

Moving to the specific wind sector of $180\pm5^{\circ}$ (Figure 2b), it is shown that only the rows 2 and 3 experience wake losses for Southerly wind directions with similar values of the percentage wake loss. Figure 2c shows the percentage power losses for wind directions $210\pm5^{\circ}$, where only certain turbines of rows 2 and 3 are affected by wakes. Finally, the wind sector with the largest percentage power loss, i.e. WD= $270\pm5^{\circ}$ is shown in Figure 2d. Due to short spacing of 3.3 d in the spanwise direction, the turbines experience a very significant percentage power loss, as high as 80% in the stable regime and 70% for the convective regime.

To characterize effects on power performance due to the variability of wind speed, direction and atmospheric stability, the cumulative power loss is estimated as individual turbine power loss normalized by the total gross AEP. Figure 3a shows the cumulative power loss for the entire wind rose. The stable regime (dashed bars) shows higher cumulative power loss, similarly to percentage power, especially for the turbines near the center of wind farm.

The prevailing southerly wind directions are investigated through the wind sectors $180\pm5^{\circ}$ and $210\pm5^{\circ}$, which are shown in Figure 3b and c, respectively. For the wind sector $180\pm5^{\circ}$, it can be observed how the wake losses affect significantly the second and third rows. According to the wind rose for this sector (Figure 1), the stable regime has higher probability of wind speeds greater than the rated speed of the turbine, while the convective regime has turbines operating primarily in region 2 of the turbine power curve. It is noteworthy that this wind sector has the highest probability of wind, for both convective and stable regimes (14% of the entire measurement period). Therefore, power losses resulting for this wind sector have a significant effect on the overall wind farm performance. Moving to the wind sector of $210\pm5^{\circ}$ in Figure 3c, the wake losses are found to be significantly lower for all the turbines, but for the turbines located in the eastern side of rows 2 and 3. The losses from convective region are found to be slightly higher, which is consistent with the occurrence of wind speeds lower that rated velocity.

Finally, wind directions from west to east, i.e. $270\pm5^{\circ}$, reported in Figure 3d shows high power losses due to the turbines in each row, which are a consequence of the alignment of the wind turbines with the mean wind direction combined with a very short spacing of 3.3 d. The power loss from the stable regime is found to be significantly higher than that for the convective regime. This result entails from the larger occurrence of this wind direction for stable conditions rather than for convective conditions, as shown in Fig. 1.

The Case 1 reported in Table 1 is considered as the baseline case for the level 1 of the optimization

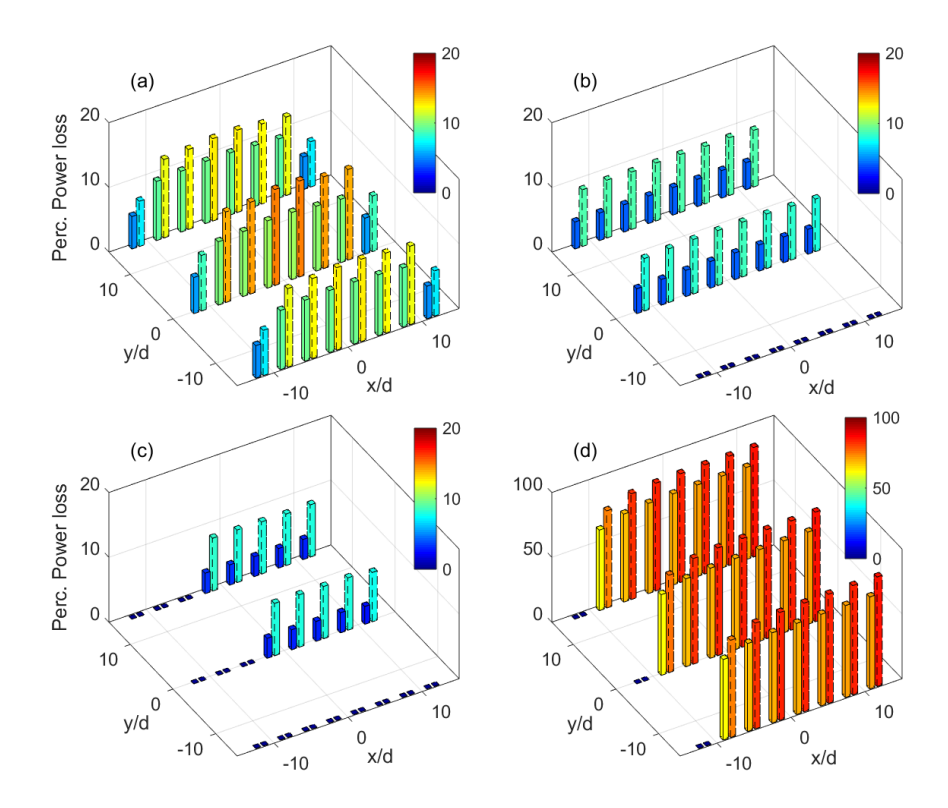


Figure 2. Percentage power loss for the convective (bars with solid lines) and stable regimes (bars with dashed lines): a) entire wind rose; b) $180\pm5^{\circ}$ wind sector; c) $210\pm5^{\circ}$ wind sector and d) $270\pm5^{\circ}$ wind sector.

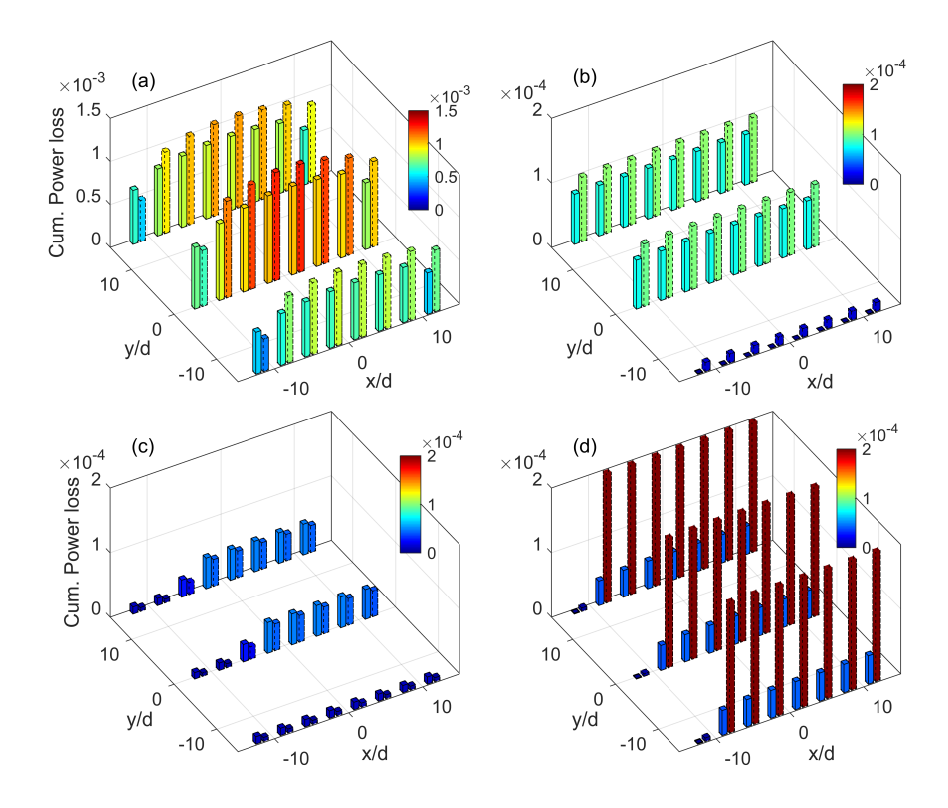


Figure 3. Cumulative power loss for the convective and stable regimes, represented by bars with solid lines and dotted lines, respectively: a) entire wind rose; b) $180\pm5^{\circ}$ wind sector; c) $210\pm5^{\circ}$ wind sector and d) $270\pm5^{\circ}$ wind sector

problem. With an LCoE of 49.34 \$/MWh for a land cost of 0.05 \$/m², this wind farm already represents high power potential for the considered site.²⁵ Case 2 represents a wind farm with 33 turbines with a smaller rated power of 1.7 MW. The total wake loss is estimated at 4.3%, which is higher than the baseline configuration. This can be reasoned with the higher number of turbines and, thus, wakes for this layout. The estimated LCoE for this case is 2.08 \$/MWh higher than for Case 1. This LCoE increase has contributions from three sources, namely capital and O&M costs (+3.7%), land costs (+10.6%) and AEP (-0.2%), as shown in Figure 4.

To further investigate the change in LCoE from Case 1 to Case 2, a new case with same layout as baseline but replacing turbine ratings from 2.3 MW to 1.7 MW is analyzed, which is denoted as Case 3. For cases 2 and 3, costs normalized per MW-power of installed capacity are expected to be the same as for the other cost parameters shown in Appendix. AEP normalized by the rated farm power for Case 3 is equal to that of Case 1 (Figure 4c); thus, it is larger than for Case 2 due to reduced wake losses as a consequence of the smaller number of turbines (24 turbines for Case 3 as opposed to 33 turbines in Case 2). Cases 2 and 3 have very similar LCoE of 51.42 and 51.30 \$/MWh, respectively; thus, the difference between Cases 1 and 2 is primarily associated with the change in capital costs for different sizes of the turbines.

Moving to Case 4 with 18, 3-MW turbines, the total wake losses are estimated to be lowered by 0.2% from the baseline Case 1, suggesting once again the cluster effect in wake interactions reduces for this configuration due to the lower number of turbines. The LCoE was estimated to be lowered by 1.56 \$/MWh having contributions primarily due to reduced total costs, while the AEP normalized by installed capacity is also found to be higher as compared to baseline case. These results are in line with the trend observed in the wind energy industry, where the average turbine size is on the rise.²³

It is concluded from the first level of optimization that the optimal configuration consists of 18, 3-MW turbines. For the second level of the optimization problem, the streamwise spacing, s, is optimized as shown in Figure 5. In addition to the land cost of $0.05 \text{ }\$/\text{m}^2$ considered for the optimization level 1, three different land cost parameters are analyzed. Indeed, this optimization level targets the trade-off between land cost and AEP to determine the optimal spacing, which is essential to represent how variations on land costs would affect the optimal spacing of the farm.

Effects on LCoE connected with land costs of $0.025 \text{ $/m^2$}$, $0.05 \text{ $/m^2$}$, $0.1 \text{ $/m^2$}$ and $0.2 \text{ $/m^2$}$ are shown in Figure 5. The percentage wake loss as a function of streamwise spacing is shown in Figure 6. The trend is seen to be similar between total wake loss and its relative contribution from losses during convective and stable regime. The total wake loss varies from 9.5% for 4-d spacing to only around 3% for 18.5-d spacing. The land cost of $0.05 \text{ $/m^2$}$ used in level 1, shows a plateau in Figure 5, suggesting a balance between increased wake losses and reduction of cost of land for a reducing streamwise spacing. The optimal spacing for this land cost was about 10 d and is within 0.3 \$/MWh of either increasing or decreasing the spacing by 3.5 d.

As the land cost increases to $0.1 \text{ }^{\circ}/\text{m}^{2}$, then the optimal spacing becomes 7.5 d. Considering this land cost, the optimal LCoE was lowered by 1 $\text{ }^{\circ}/\text{MWh}$ compared to the baseline spacing of 14.5 d. The case with the highest land cost of $0.2 \text{ }^{\circ}/\text{m}^{2}$, shows the maximum potential for LCoE optimization. The wake loss increases by 3.5% moving from 6.5 d spacing to 4.0 d, indicating the significance of detrimental wake effects on power production for wind farms with closely-spaced turbines.

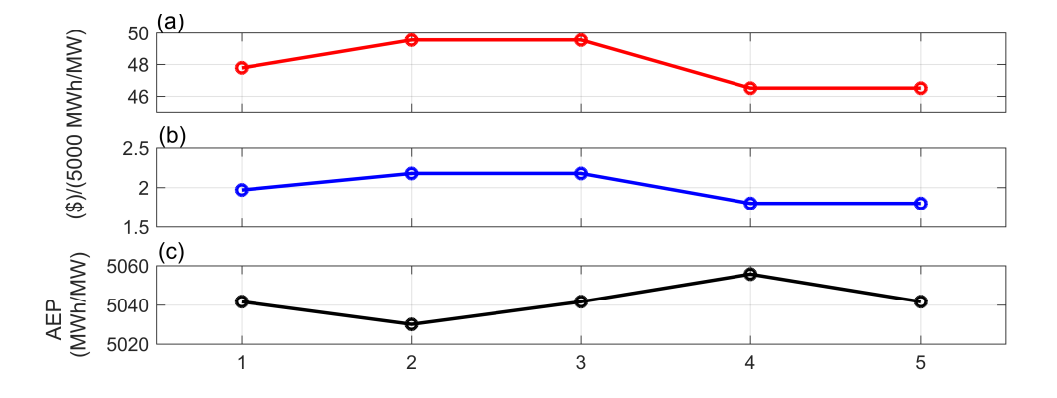


Figure 4. Contribution to LCoE from: a) capital, operation and maintenance costs; b) land costs and c) AEP; for different wind farm cases reported in Table 1.

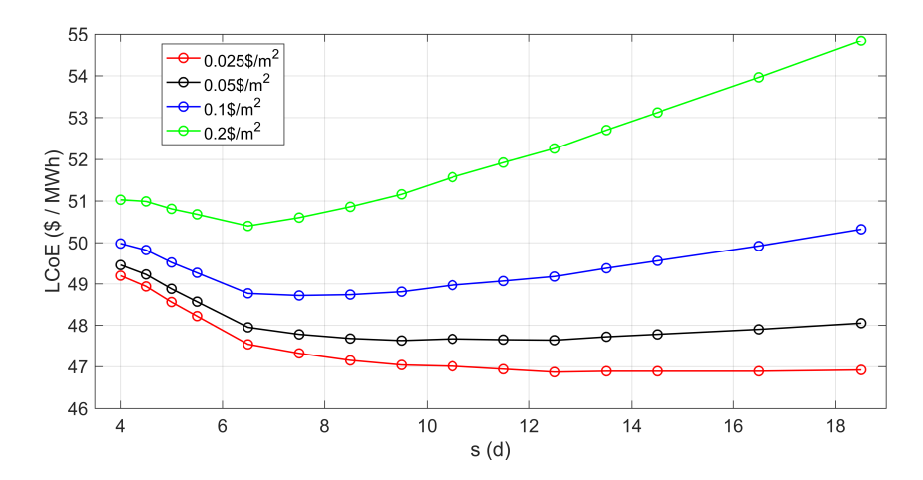


Figure 5. LCoE from level 2 of the optimization problem, where uniform spacing between turbine rows, s, is optimized for different land costs.

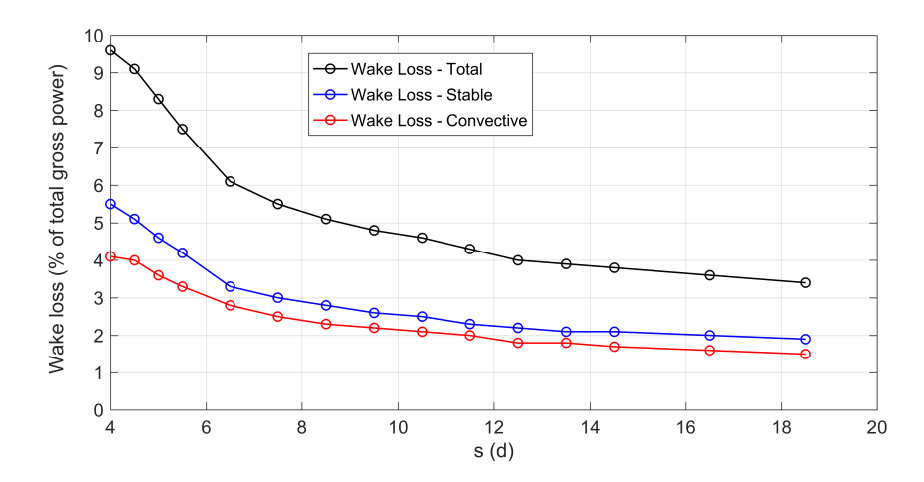


Figure 6. Wake loss as percentage of the gross AEP for different streamwise spacing between turbine rows and atmospheric stability regimes for the wind farm configuration of 18, 3-MW turbines.

The trends for different costs of land, as reported in Figure 5, plays an important role in the outcome of the optimization problem, especially for spacing greater than $6.5\ d$. Furthermore, this result also suggests that although the level 2 of the optimization targeted losses in the main wind sector between 150° to 210° , a significant source of the total wake loss for $14.5\ d$ spacing occurs from the wake interactions between the spanwise turbines, as shown in Figure 3d.

V. Conclusions

A RANS-based model is used to simulate the intra-wind-farm wake flow for a design optimization problem. This RANS solver allows predicting wind turbine wakes, wake interactions and their effects on power capture for different atmospheric stability conditions, namely stable and convective regimes. The design optimization of a relatively small wind farm, which is the archetype of a real onshore wind farm located in North Texas, has been performed with a two-level problem by utilizing as input meteorological data for the site under investigation.

The first level of the optimization problem consists in determining the optimal capacity of the wind farm, i.e. rated power and total number of the turbines. It has been shown that according to the wind resource of the site under examination, the optimal configuration consists of 18, 3-MW wind turbines entailing an LCoE of 1.56 \$/MWh lower than the configuration with 24, 2.3-MW turbines, which is similar to that of the real wind farm.

The optimization of the uniform spacing between the turbine rows for this configuration has been found to be sensitive to the land cost. Varying the land costs between values of 0.025 s/m^2 , 0.05 s/m^2 , 0.1 s/m^2 and 0.2 s/m^2 , optimal ranges in spacing of $12 \leq s/d \leq 18$, $9 \leq s/d \leq 13$, $6 \leq s/d \leq 9$ and $5.5 \leq s/d \leq 7.5$, respectively, have been obtained. Spacing turbines closer than 5.5 d results in drastic wake losses, which are larger than the respective reduction in cost of land. For the land cost of 0.1 s/m^2 , the results obtained from the two levels of the optimization could reduce the LCoE by 2.5 s/MWh from the existing wind farm, which would translate to approximately \$700,000 per year in cost for the wind farm under examination. Future research should include varying the spanwise spacing and exploring the potential of a non-uniform spacing as the third level of the optimization problem.

Acknowledgments

The Texas Advance Computing Center is acknowledged for the computational time.

Appendix

In this Appendix, the cost model for onshore wind farms is broken down to each individual cost component. The first contribution to the costs is represented by the cost of electrical infrastructure for the j-th turbine, $C_{elec,j}$, and the capital cost, $C_{wt,j}$, including turbine components, such as tower, foundation and rotor-nacelle assembly. The capital cost can be further broken down into the following components:

- Rotor and Nacelle Assembly Cost, C_{RNA} = 929 $\times P_{rated}$
- Tower Structure Cost, C_{Tower} =4.42 $\left(0.016\ d^{2.8}\left(\frac{z_h}{d}\right)^{1.7}\left(\frac{P_{rated}}{A}\right)^{0.6}\right)$
- Tower Foundation Cost, $C_{Fo} = 523.77 \left(\frac{\pi}{4} z_H d^2\right)^{0.4}$
- Assembly and Installation Cost, $C_{A\&I} = 2.09(z_H d)^{1.17}$
- Miscellaneous Costs, C_{misc} : Engineering Management = 1.1% of capital cost Development = 0.9% of capital cost Site access and Staging = 2.8% of capital cost Construction Financing = 2.9% of capital cost Contingency = 6.0% of capital cost
- Electrical Infrastructure Cost, $C_{elec} = 1.86 \ P_{rated} \left(3.49 \times 10^{-6} P_{rated}^2 0.0221 P_{rated} + 109.7 \right)$

where P_{rated} is the turbine power rating, d is the rotor diameter, z_h is the hub height, and A is the rotor swept area. The original cost model in Ref.²² was corrected for inflation and to depict the costs for onshore wind farms in the year 2015 reported in Ref.²¹ In this work a value of 12% is considered for the FCR to reflect realistic LCoE for the site under examination.

The second portion of the cost in LCoE is represented by annual cost associated with operation and maintenance of the wind farm. The operation and maintenance costs are described as: $C_{oper} = 15 \times P_{rated}$ and $C_{main} = 28 \times P_{rated}$ [\$/kW], respectively.²¹ In addition, the land leasing cost is also part of this cost. The land cost component, $C_{land} = c_{land} \times A_{farm}/N_w$, where A_{farm} is the total farm area, N_w is the total number of turbines in the farm, and C_{land} is a land cost coefficient (\$/m^2). c_{land} was derived using the NREL reference case consisting of 100 turbines arranged in ten rows with ten turbines each. Since the reference farm layout is not specified, an assumption was made for the spacing. Specifically, 8-d spacing is assumed between two rows, while the spanwise spacing was assumed to be 4 d. Using the cost of land value reported, the land cost per unit area was estimated to be 0.05 \$/m^2.

References

- ¹Herbert-Acero, J., Probst, O., Réthoré, P.-E., Larsen, G. C. and Castillo-Villar, K. K., "A review of methodological approaches for the design and optimization of wind farms," Energies, Vol. 7, 2014, 6930-7016.
- ²Mosetti, G., Poloni, C. and Divacco, B., "Optimization of wind turbine positioning in large wind farms by means of a genetic algorithm," J. Wind Eng. Industr. Aerodyn., Vol. 51, 1994, 105-116.
- ³El-Asha, S., Zhan, L. and Iungo, G.V., "Quantification of power losses due to wind turbine wake interactions through SCADA, meteorological and LiDAR data," Wind Energy, Vol. 20, 2017, 1823-1839.
 - ⁴Jensen, N., "A note on wind generation interaction," Tech. Report, 1983, Ris-M-2411.
- ⁵Bastankhah, M. and Porté-Agel, F., "A new analytical model for wind-turbine wakes," Renewable Energy, Vol. 70, 2014, 116-123.
 - ⁶Troen, I. and Petersen, E.L., "European wind atlas." Roskilde: Riso National Laboratory, 1989.
- ⁷Iungo, G.V., Santhangopalan, V., Ciri, U., Zhan, L., Viola, F., Rotea, M.A. and Leonardi, S., "Parabolic RANS solver for low-computational-cost simulations of wind turbine wakes" Wind Energy, 2017, 1-14, doi.org/10.1002/we.2154
- ⁸Santhanagopalan, V., Rotea, M. A. and Iungo, G. V., "Performance optimization of wind turbine column for different incoming wind turbulence," Renewable Energy, Vol. 116, Part B, 2017, 232-243.
- ⁹Iungo, G. V., Viola, F., Ciri, U., Rotea, M. A. and Leonardi, S., "Data-driven RANS for simulations of large wind farms," J. Phys.: Conf. Ser., Vol. 625, 2015, 012025.
- ¹⁰Iungo, G. V., Viola, F., Ciri, U., Leonardi, S. and Rotea, M. A., "Reduced order model for optimization of power production from a wind farm," AIAA SciTech, 34th Wind Energy Symp., 2016, AIAA 2016-2200.
- ¹¹Machefaux, E., Larsen, G.C. and Leon, J.M., "Engineering models for merging wakes in wind farm optimization applications," J. Phys.: Conf. Ser., Vol. 625, 2015, 012037.
- ¹²Katic, I., Hjstrup, J. and Jensen, N.O., "A simple model for cluster efficiency," European Wind Energy Ass. Conf., 1986, 407-410.
 - ¹³Hall, M., "Vortex breakdown," Annual Rev. Fluid Mech., Vol. 4 (1), 1972, 195-218.
 - ¹⁴Pope, S. B., "Turbulent flows," Cambridge Univ. Press, 2000.
- ¹⁵Jonkman, J., Butterfield, S., Musial, W. and Scott, G., "Definition of a 5-MW reference wind turbine for offshore system development," NREL Tech. Report, National Renewable Energy Laboratory, 2009.
 - ¹⁶Mikkelsen, R., "Actuator disc methods applied to wind turbines," PhD thesis, Technical University of Denmark, 2003.
- ¹⁷Shen, W., Sorensen, J. N. and Mikkelsen, R., "Tip loss correction for actuator/Navier-Stokes computations," J. Sol. Energ.- T. ASME, Vol. 127, 2005, 209-213.
- ¹⁸Shen, W., Mikkelsen, R., Sorensen, J.N. and Bak, C., "Tip loss corrections for wind turbine computations," Wind Energy, Vol. 8, 2005, 457-475.
- ¹⁹Stevens, R. J., Hobbs, B. F., Ramos, A., and Meneveau, C., "Combining economic and fluid dynamic models to determine the optimal spacing in very large wind farms." Wind Energy, Vol. 20, 2017, 465-477.
- ²⁰Wharton, S. and Lundquist, J.K., "Atmospheric stability affects wind turbine power collection." Environ. Res. Lett., Vol. 7, 2012, 014005.
- 21 Mon, C., Hand, M., Bolinger, M., Rand, J., Heimiller, D. and Ho, J., "2015 Cost of wind energy review." NREL/TP-6A20-66861, 2017.
 - ²²Fingersh, L., Hand, M. and Laxson, A., "Wind turbine design cost and scaling model." NREL/TP-500-40566, 2006.
- ²³Wiser, R., Jenni, K., Seel, J., Baker, E., Hand, M., Lantz, E. and Smith, A., "Expert elicitation survey on future wind energy costs." Nature Energy, 1, 2016, 16135.
- ²⁴Iungo, G. V. and Porté-Agel, F., "Volumetric lidar scanning of wind turbine wakes under convective and neutral atmospheric stability regimes," J. Atmos. Ocean. Tech., Vol. 31 (10), 2014, 2035-2048.
- ²⁵Wiser, R.H. and Bolinger, M., "2016 Wind technologies market report", Lawrence Berkeley National Lab., 2017, LBNL-2001042.